International Journal of
INTELLIGENT SYSTEMS AND APPLICATIONS IN ENGINEERING
ISSN:2147-6799 www.ijisae.org Original Research Paper

Cad System for the Detection and Classification of Alzheimers from MR Images Using Deep Learning Techniques

Nithya V. P.[1], Dr. N. Mohanasundaram[2] and Dr. R. Santhosh[3]

Submitted: 21/08/2022 **Accepted:** 23/11/2022

***Abstract*:**Alzheimer's disease, also known as Alzheimer's degeneration, is an irreversible brain disorder affecting over 65-year-olds.AD cannot currently be cured, but its progression can be slowed by certain treatments.It is imperative to diagnose AD accurately and early to improve patient care and future treatment options.Many ways evaluate picture features to retrieve handmade characteristics and then design a classifier to differentiate AD from other groups. The Alzheimer's Disease Neuroimaging Initiative (ADNI) dataset is used to propose a new method for categorizing AD and MCI.Preprocessing of brain pictures, including image segmentation, is essential for these methods.To reduce noise and factor fluctuations, the pictures are preprocessed using several complex methods.The preprocessed images are then used to segment the images.This study presents a novel classification algorithm based on deep learning and ResNet 50, inspired by deep learning's success in image analysis.The suggested classifier approach allows the selection of relevant characteristics while avoiding overfitting issues.When the proposed algorithm was compared to the existing models, the results proved that it had better accuracy values.

Keywords: *CLAHE, BADF, K-means clustering, ResNet 50.*

1. Introduction

The alarming statistics about the prevalence of AD are also an important factor for focusing the attention on predicting and finding AD patients. Alzheimer's disease, a chronic neurological illness, causes irreversible cognitive function loss and dementia. There is no cure for this ailment, and its aetiology is unknown. According to Alzheimer's disease facts and numbers 2022 [1], 6.5 million senior citizens will have Alzheimer's disease in 2022.They're all over 75, with 73% of them being over 75. Alzheimer's disease can affect around one out of every nine seniors over the age of 65. (10.7 per cent).The report is also giving alarming information about the high mortality rate of AD patients, especially among the aged population around the globe. The presence of AD can make a significant negative impact on the health of an aged person who is already suffering from other severe diseases. However, the report emphasizes the early detection of AD for helping the physicians cope with this because it helps them in designing appropriate and better medication strategies like prescribing appropriate drugs for reducing the rate of progression of AD [2]. Moreover, the related family and friends of the AD patient can give better care to them. Such pre-planned strategies improve the quality of life of an AD patient even in their old age. Along with this, classifying the cognitive impairment of the patients in advance helps the physician provide the required and optimal treatment for dealing with the disease. Figure 1 shows the existence of AD on neuron cells.

Figure 1: Neurons in the brain display microscopic plaques and tangles in Alzheimer's illness

Computer-aided systems are very helpful in diagnosing medical images, which is otherwise a difficult task.The most popular imaging techniques for diagnosing neurodegenerative disorders include Computer Tomography (CT), Magnetic Resonance Imaging (MRI), and positron emission tomography (PET). Among these, CT scanning takes a shorter time and the images are clearer.Various diseases can be examined using CT scanning.MCI(Mild Cognitive Impairment), could be mistaken for a natural result of ageing due to its limited resolution in the middle lobe.With Pet, you'll get improved sensitivity and resolution, and your images won't be absorbed by tissue, as there is no tissue absorption [3].The inside architecture of the human body is imaged using an MRI scanner. With a rapidly changing gradient magnetic field, MRI can be speeded up significantly, and good soft tissue resolution can be achieved

[1]*Research Scholar, Department of Computer Science and Engineering, Karpagam Academy of Higher Education,Coimbatore, Tamil Nadu, India, nithyaharisree@gmail.com*
[2] *Professor, Department of Computer Science and Engineering,Faculty 0f Engineering, Karpagam Academy of Higher Education, Coimbatore,Tamil Nadu, India, itismemohan@gmail.com*
[3]*Professor, Department of Computer Science and Engineering,Faculty 0f Engineering, Karpagam Academy of Higher Education, Coimbatore,Tamil Nadu, India, santhoshrd@gmail.com*

without ionizing radiation.In picture analysis, feature extraction plays a crucial role.Several previously studied regions such as the amygdala, hippocampus and other brain regions must be manually removed [4].Because manual labour is required, there are restrictions as well as the possibility of human error. Because of the rapid advancement of artificial intelligence, computer vision has become increasingly crucial in diagnosing Alzheimer's disease. Deep learning is a popular machine learning branch that can solve problems that old techniques can't. In recent times, deep learning technology has dominated medical imaging, and it has been effectively employed to extract the features from medical pictures to identify Alzheimer's illness [5]. Alzheimer's illness is anticipated to grow more widespread by 2022, according to Figure 2 of Alzheimer's illness Facts and Figures, 2020.

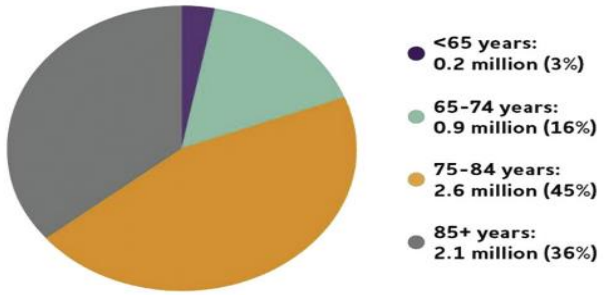

Figure 2. In Alzheimer's illness Facts and Figures, 2022, the prevalence of Alzheimer's illness is reported.

Importance of DL algorithms in AD classification

DL algorithms are used to get more insights from the health care data [6]. Likewise, the application of DL algorithms helps a physician by assisting in the crucial decision-making process for distinguishing MCI (Mild Cognitive Impairment), AD, and HC (Healthy Controls) [7]. The Healthy Controls (HC) are the individuals who do not have any cognitive impairment. However, some HCs would have Mild Cognitive Impairment (MCI) at some stage of their life. MCI is a state of cognitive impairment where the individual can do daily activities like bathing, and brushing without difficulty, but, MCI patients face difficulty in solving logical problems, and recalling historical or past events. As the exact reasons responsible for developing AD is unknown, the physician infers whether the patients are most likely to develop AD or MCI after observing the characteristics that are related to MRI, PET, SPECT medical images, cognitive memory assessment tests, CSF and demographic data. However, this is a challenging task for physicians because it is difficult to find a pattern between the MCI and AD patients after observing these data [8]. This is where DL algorithms are deployed on these characteristic data of the patients for finding the hidden patterns and crucial features that are playing a major role in distinguishing MCI, AD, and HC. The DL algorithms make use of information from various other domains such as statistics and mathematics to accomplish this. Thus, the overall application of the DL algorithm in the AD domain makes a good impact on the physician in assisting them.

2. Literature Review

Since picture acquisition is done by machines made by various manufacturers, the medical staff's operation procedures may vary. Furthermore, due to the lengthy acquisition time, the subject's physique will certainly change to some degree. To get the actual picture, a series of preprocessing processes must be done to satisfy the demand for feature extraction, feature selection, and classification.Preprocessing is essential before data operations in most studies, particularly in machine learning. Some research may not require preprocessing if deep learning is used. The majority of the research still uses raw data preprocessing processes such as intensity normalization, registration, skull dissection, and motion correction [9,10].

Researchers Gao and Lio [11] examined deep learning algorithms for detecting Alzheimer's illness. The authors described biomarkers and features for detecting the disease, as well as methods for detecting it.As per the research, deep learning technology is effective for detecting Alzheimer's.Heba et al. [12] employ deep learning methods to identify END. The system is made up of four different processes: transfer learning, deep feature extraction, feature reduction, and classification. The fusion of features is crucial to the framework's success.A method of analyzing embryonic MRI images at various gestations was found to be effective at diagnosing ENDs (embryonic neuro-developmental disorders).The results are then compared to comparable studies that employed embryonic photos to confirm the efficacy of the suggested framework.The proposed application's efficiency was comparable to that of other frameworks. As a result, the proposed framework may be utilized to detect END in a step-by-step fashion. For AD prediction, Fei et al. [13] build a deep CNN based on a multiple attention approach. First, cyclic convolution is used to improve the feature information in the MRI picture. Second, a multiple attention technique is used to re-calibrate features and adaptively learn feature weight to discover brain regions that are particularly important for disease detection. Lastly, for the backbone network, an enhanced VGG model is given. The accuracy, sensitivity, and specificity of AD prediction are all 99.8%, 99.9%, and 99.8%, respectively, according to the trial.Loddo et al. [14] conducted Alzheimer's disease studies and research using computer-aided diagnosis while assessing numerous deep learning models (CAD). Based on patient brain scans, the suggested method is designed to give significant support for clinical care.

Problem Statement

The major challenge faced in AD classification is preprocessing and feature extraction which results in an inaccuracy classification of MRI images. The existing methods provide inaccurate results in segmentation as well as feature selection. Also, it has a problem along with computational complexity due to the number of iterations. Thus, the overall MRI classification performance is reduced significantly. Consequently, advanced methods for the removal of noise from MRI images were developed, including preprocessing, feature extraction, feature selection, and classification.

The objective of the Research

The primary goal of this study is to create and implement automated multiclass diagnostic detection techniques on MRI scan pictures using image processing and data mining.The major objectives of this research work have been:

- To study in detail, research on Alzheimer's Disease & Image Processing.

- To analyze the existing Algorithms for detecting Alzheimer's Disease from MRI Images.
- To develop an algorithm for preprocessing the MRI images for the Noise Removal.
- To design & develop an algorithm for effective classification of Alzheimer's Disease.
- To maximize the performance measures of Preprocessing and Classification of Alzheimer's Disease.
- To determine the most effective improved picture for Alzheimer's disease detection.

The following sections provide the framework for the paper: Alzheimer's disease is explained in part 1 as an introduction. The literature reviews are explained in part 2, and the planned study is presented in part 3. The result analysis is presented in part 4, and the work is concluded in part 5.

3. Proposed Work

A computer-assisted automatic detection system is offered as a way of detecting Alzheimer's disease. Figure 3 depicts the whole detection technique. The original MRI picture is first preprocessed, after which it is improved using CLAHE and BADF, and finally turned into K-means clustering. The neural network classifier is then trained using deep learning-based ResNet 50 structures to identify the picture as normal or abnormal, using the trained characteristics as a guide. Finally, the MRI image categorization system's performance is evaluated.

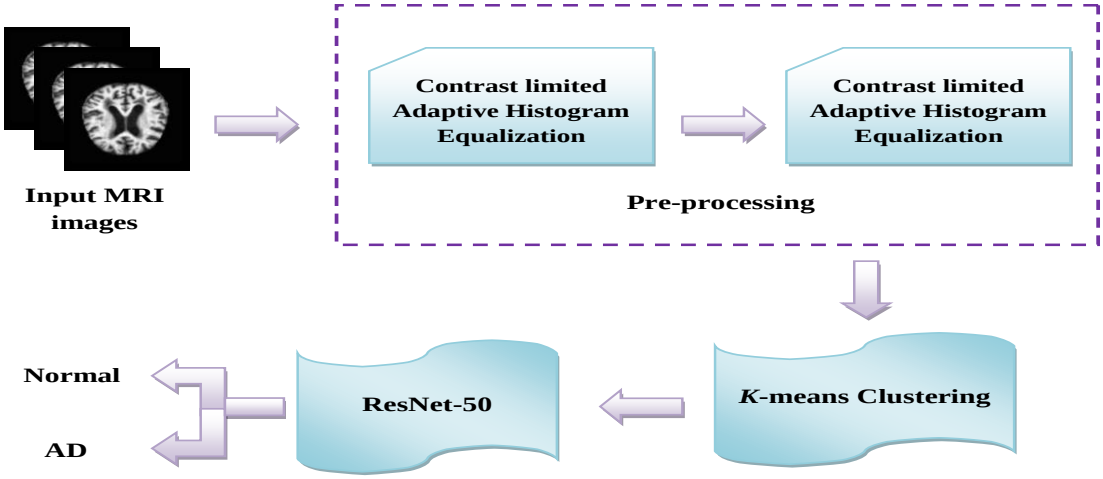

Figure 3: Overall Block Diagram

a. Preprocessing

Pre-main processing's goal is to improve the picture's uniformity. It removes or minimizes non-related and unnecessary components in medical data to prepare them for subsequent processing.

Contrast Limited Adaptive Histogram Equalisation

In the first place, CLAHE was designed to aid in low-contrast medical imaging.Regular AHE has different limitations.Noise amplification was combated by implementing clipping limitations on the CLAHENoise amplification was combated by implementing clipping limitations on the CLAHE.There are multiple contextual components in the CLAHE picture, including sub-images, tiles, and blocks. Two parameters are critical in CLAHE: the Block Size (BS) and Clip Limit (CL).Image quality is determined by these two variables.Due to the low intensity of the input picture and the flattening effect of a larger CL, the picture appears brighter as CL is increased.This dynamic range and visual contrast increase as the BS grows larger. With the entropy of the picture [15, 16], the two factors set at the place with the greatest entropy curvature give subjectively good picture quality.

The phases in the CLAHE approach for enhancing the actual photo are as follows:

Step 1: By converting the original pixel intensity into non-overlapping contextual zones.MN refers tothe "total number of image tiles," and an 88 percent figure is optimum for preserving chromatic knowledge in photographs.

Step 2: Depending on the grey scale in the above photo, make a histogram for each contextual area.

step 3: The contrast restricted histogram of the platform can be calculated based on the CL score.

$$N_{avg} = (NrX \times NrY)/N_{gray} \quad (1)$$

N_{avg} is the average number of pixels in the platform,N gray is the number of grayscale pixels, and NrX and NrY are the pixels per direction in the platform.

Step 4: Re-distribute the remaining pixels until none remain. The following formula is used to determine the redistributing pixel stage:

$$step = N_{gray}/N_{remain} (2)$$

N_ pixels are still cut.A step is a one-digit positive integer. The value indicates how many snipped pixels were left. A phase is an integer that is at least one. Whilethe system scans from the lowest to the highest grey level, as it did in the previous step,the software will add one pixel to grey levels that are less than N CL.If there is unequal dispersion of pixels at the end of the research, the algorithm will calculate a new path using Eq.(2) and repeat the lookup until all leftover pixels are evenly scattered.

Step 5: Each region's brightness distribution is boosted by the Rayleigh transform.The accumulated probability $P_{input}(i)$function is employed on the trimmed histogram.When the Rayleigh distribution is utilized, the underwater picture

looks to be more natural. The forward transform of Rayleigh is calculated as follows:

$$y(i) = Y_{min}\sqrt{2\alpha^2 ln\left(\frac{1}{1-P_{input}(i)}\right)} \qquad (3)$$

Where Y min is the pixel value's lower bound, and α is a Rayleigh distribution scaling parameter that is determined by the input image. The Rayleigh function has an α value of 0.04 in this investigation. For each brightness point, the outcome probability density is:

$$P\big(y(i)\big) = \frac{y(i)-Y_{min}}{\alpha^2} exp\left(-\frac{(y(i)-Y_{min})^2}{2\alpha^2}\right) \quad for y(i) \geq Y_{min} \quad (4)$$

A greater number will give in more significant picture contrast enhancement while also raising saturation and noise levels.
Step 6: Mitigating the effect of a sudden change, Linear intensity stretch is used to rescale the result of the transfer function in Eq (9). The linear contrast stretch is calculated as follows:

$$y(i) = \frac{x(i)-x_{min}}{x_{max}-x_{min}} \qquad (5)$$

The transfer function's lowest and maximum variables are x_{min} and x_{max}respectively, and input data for this function is x(i).
Step 7: The grey scale distribution of pixels within a sub-matrix system can be calculated using a bi-linear interpolation of four separate mappings to remove border artefacts.

Boosted Anisotropic diffusion filter

By maintaining fine details in the image, it primarily focuses on removing noise. After obtaining the scattered picture, this BADF includes the Partial Differential Equation (PDE), which gives the anisotropic scattering filter [17] an extra advantage. A type of diffusion that is lacking at the edges and borders can also be used to smooth the surface.

The smoothing scheme in anisotropic filtered is based on the PDE regulating system.

$$\frac{\partial I_m}{\partial t} = div(T\nabla I_m) \qquad (6)$$

I_m is for image intensity, ∇ stands for gradient, div stands for dispersion, and T stands for time in the weighting direction. Smoothing orientation is determined by the structure tensor T. It is constructed using a common gradient tensor G, which is obtained by correlating the total of outer ∇Im goods with a Gaussian kernel Kρ across all weighted instructions:

$$G = k_p * \sum_m (\nabla I_m \oplus \nabla I_m) \qquad (7)$$

The outer product operator is represented by ⊗. The gradient tensor's spatial scale is ρ, determined by the standard deviation of the Gaussian kernel. An anisotropic diffusion filter's main benefit is that it smooths out the image's homogeneous sections while also enhancing the edges.
While Gaussian filters function well in many practical uses, they are significantly constrained when the true state distribution is complicated, such as when there are several modes, high skewness, or large tails. In multi-target tracking or financial forecasting, for example, such circumstances may develop. The obvious extension of Gaussian filtering is Gaussian mixture filtering, which provides a consistent filter in various situations. Both the expected and posterior densities of the state are considered to be Gaussian mixes when using a Gaussian mixture filter.

$$f_k^*(x_k) = \sum_{i=1}^{L_k^*} \omega_{k,i}^* . N\big(x_k; x_{k,i}^*, C_{k,i}^*\big), with * \in [e,p] \qquad (8)$$

L_k^* is the number of mixture components for every time step is k.

b. Segmentation

Medical image segmentation, also known as natural image segmentation, is the process of manually, semi-automatically, or fully automating the extraction of the desired object (organ) from a medical image (2D or 3D). In a variety of applications, medical picture classification is crucial. Microscopy, dermoscopy, X-ray, ultrasound, Computed Tomography (CT), Magnetic Resonance Imaging (MRI), and positron emission tomography are just a few of the imaging techniques that have recently gotten a lot of attention and funding. One of the most significant medical imaging techniques is picture segmentation, which retrieves the ROI using a semiautomatic or automatic process. It used border identification, tumor tracking, and mass recognition in clinical uses to segment body organs and tissues.Because classification divides a picture into logical sections, clustering algorithms can be used to professionally separate the ROI from the background by extracting the image's global properties [18].

- ***K-means Clustering***

K-means is a clustering method or strategy that quickly and easily organizes a massive quantity of information [19].In contrast, the k-means algorithm relies on the initial cluster of values to locate the centre and thus has a flaw.K- means clustering produces optimal topical treatments as an outcome of the trials. The testing process, on the other hand, should result in data similarities or proximity. As a result, it can be divided into multiple clusters, each with a high degree of similarity among cluster locations. As cited by (celebi et al. 2013), K-Means is a multifaceted approach due to the ease with which it can be modulated at each stage, the ease with which it can quantify distance, and its reliance on iteration termination criteria.The beginning parameters obtained from the cluster's midpoint are significant because the K-mean cluster is a local optimization.These changes are made to attain the highest accuracy and quickest convergence. Furthermore, starting from a cluster's midway limits the K-mean cluster method to the best possible site. The k-mean cluster method chooses a beginning point from the centre at randomized from a range of styles up to k. Based on the original centroid cluster, which is selected at random, the number of iterations with the centroid cluster is determined. As an outcome, the centroid cluster in the large starting data points can be improved. Data points [1,2,3,...,x] n are typically clustered into k-means using k-means clustering.It supports multi-dimensional vectors and features high-performance computing. Figure 4 depicts the flow chart of K-means clustering. As a result, the distortion measure is reduced by lowering the cost function, which includes:

$$\left|x_i^j - c_j\right|^2 \qquad (9)$$

The x_i^j metric is used to calculate the distance between both the cluster centre and a piece of data.(n) data points are measured by (c_j) from their cluster centres.The following parts make up the algorithm:

1. Set the k points in the clustered object's space. These are the initial C_ k centroids.

$$\boldsymbol{d} = \|\boldsymbol{P}(\boldsymbol{x},\boldsymbol{y}) - \boldsymbol{C_k}\| \qquad (10)$$

2. Allocate each object's group to the subcategory with the most nearby centres.
3. While all objects are allocated, compute the locations of the k centroids.

$$\boldsymbol{C_k} = \frac{\boldsymbol{1}}{\boldsymbol{k}} \sum_{\boldsymbol{y}\in \boldsymbol{C_k}} \sum_{\boldsymbol{x}\in \boldsymbol{C_k}} \boldsymbol{P}(\boldsymbol{x},\boldsymbol{y}) \qquad (11)$$

4. Keep repeating steps 2 and 3 till the centroids stop moving.

The K-means clustering algorithm has two well-known attribututes in which minimal attributes are divided into groups

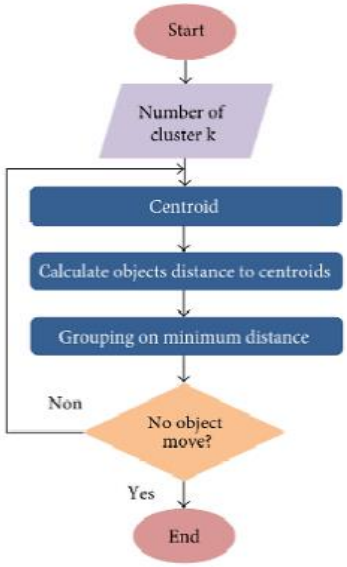

Figure 4: steps of k-means clustering

c. Deep learning technique using ResNet

Due to the introduction of new technology, the field of computer vision has seen significant changes in recent years. As a result of these improvements, computer vision models can now outperform humans in tackling many tasks such as picture identification, object detection, face recognition, image categorization, and so on. Deep convolutional neural networks, sometimes known as CNNs, need special consideration. For accurate analysis of visual imagery, artificial networks are widely used [20].However, while it allows us to add more layers to the CNNs to perform increasingly difficult computer vision tasks, it also introduces its own set of problems. It has been found that as the number of added layers increases, training neural networks gets more challenging, and the accuracy of the neural networks decreases. The use of ResNet becomes critical in this situation. Deep neural networks are more complex to learn. Resnet has made it possible to train incredibly deep neural networks without trouble.

"Residual Network" refers to the system that isn't connected to everything else. Kaiming He, Xiangyu Zhang, Shaoqing Ren, and Jian Sun initially illustrated it in their 2015 computer vision study entitled "Deep Residual Learning for Image Recognition." The groups that took first place in the ILSVRC 2015 classification competition with a 3.57 percent error rate demonstrated that this approach was a huge success. ImageNet identification, ImageNet localization, COCO detection, and COCO segmentation were all first place winners in the 2015 ILSVRC and COCO contests. ResNet is available in many different forms, each with a varied number of nodes but the same underlying concept.Resnet50 [21] is a variation that supports up to 50 neural network layers.

Deeper convolutional neural networks are used by machine learning engineers to solve an issue in computer vision since of Resnet's significance. Since the individual levels can be taught for various jobs to generate accurate results, these extra stages aid in the speedier resolution of complex problems. While increasing the number of stacks can improve the model's characteristics, a deeper network can cause performance reduction. To put it another way, as the number of channels increases, a neural network's accuracy rates may get saturated and begin to decline. As a result, both the training and testing data accuracy of the model degrades. Overfitting isn't to blame for such deterioration. It could otherwise be owing to the network's initialization, optimization algorithm, or, more crucially, the issue of vanishing or ballooning biases [22].This is why ResNet was created. Deep residual networks add residual blocks into the model to increase their accuracy. Skipping interconnections can be done in two ways. They start by generating a new path for the gradient to follow, which solves the problem of vanishing gradients. They also give the algorithm the ability to learn a function that defines its identity. As a result, the model's upper layers operate just as well as its bottom layers.So, to conclude, residual blocks simplify the layers' learning of identity values. ResNet improves deep neural network performance in addition and more neural levels with minimizing failure rates. To put it differently, skip connections mix the results of the preceding layer with the outcomes of stacked layers, enabling the training of far deeper networks than was previously available.

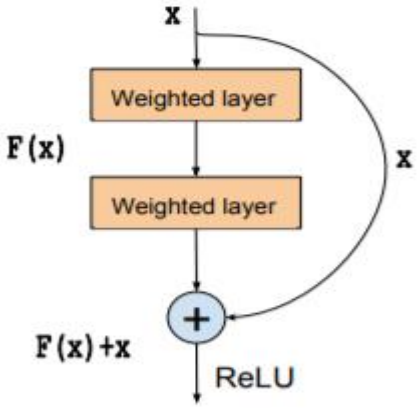

Figure 5: An illustration of a Residual block presented by (He et al. 2016), with x as the input and F(x) + x as the output, is shown before the rectified linear unit (ReLU).

As the number of layers stacked increases, the number of "levels" of attributes increases Deep networks extract small, middle, and high-level attributes.The network is built using the leftover block. A macro-architecture is formed by a series of convolutions and pooling layers. The entire architecture, as well as the description of this block, was published by (He et al. 2016). They showed that using the typical Stochastic Gradient Descent (SGD) optimizer and residual blocks, extraordinarily deep networks can be trained. As indicated in figure5, ResNet50's architecture is divided into four parts. Pictures with heights and widths multiples of 32, as well as a channel width of three, can be handled by the network. For simplicity, we'll suppose that the input size is 224 x 3. Each ResNet design uses kernel sizes of 7x7 and 3x3, respectively,

for initial convolution and pooling.In Phase 1, there were three Residual blocks, each with three levels.

Table 1. ResNet-50 architecture elements

Layer Names	Output size	Layers
Conv1	112×112	7×7, 64, stride 2
Conv2_x	56×56	3×3 max_pool, stride 2
		$\begin{bmatrix} 1\times1, & 64 \\ 3\times3, & 64 \\ 1\times1, & 256 \end{bmatrix} \times 3$
Conv3_x	28×28	$\begin{bmatrix} 1\times1, & 128 \\ 3\times3, & 128 \\ 1\times1, & 512 \end{bmatrix} \times 4$
Conv4_x	14×14	$\begin{bmatrix} 1\times1, & 256 \\ 3\times3, & 256 \\ 1\times1, & 1024 \end{bmatrix} \times 6$
Conv5_x	7×7	$\begin{bmatrix} 1\times1, & 512 \\ 3\times3, & 512 \\ 1\times1, & 2048 \end{bmatrix} \times 3$
	1×1	Avg_pooling, 1000-d fully-connected, softmax

Each of the three levels of stage 1's block uses 64, 64, and 128-bit kernels to accomplish the convolution operation. Curved arrows show the identity relationship. Dashed linking arrows indicate that the Residual Block performs the convolution operation with stride 2 (half its height and width while doubling its width) during the convolution phase.By the end of the process, the input size has been halved and the channel width has been doubled.Bottleneck design is used for deeper networks, such as ResNet50 and ResNet152.The residual function F is layered three times.The three layers are made up of 11%, 33%, and 11% convolutions. The downsizing and restoration of proportions are handled by the 11 convolution layers. The 33rd stage becomes a bottleneck as input/output dimensions decrease. Lastly, the network has a 1000-neuron fully connected layer and an Average Pooling layer (ImageNet class output). The architecture of ResNet 50 is shown in figure 6.

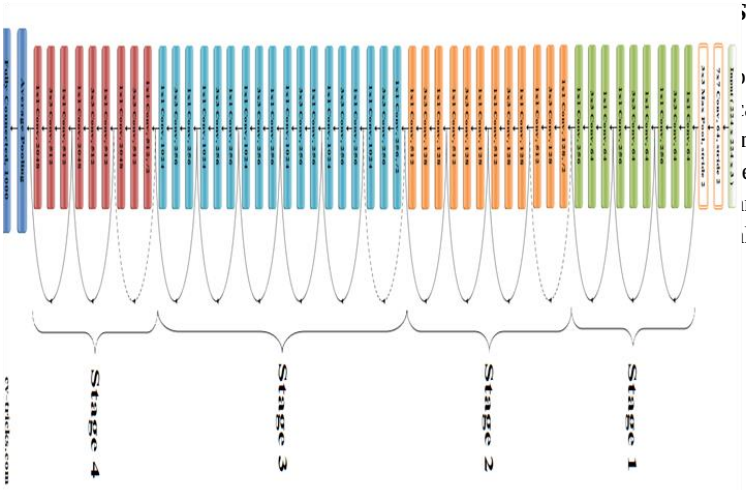

Figure 6: Architecture of ResNet-50

The ResNet-50 model, in particular, is made up of five phases, each having a residual block. Each residual block is made up of three layers with 1×1 and 3×3 convolutions. Residual blocks are a basic concept. Each layer of classic neural networks feeds onto the next. An identification network with residual blocks feeds directly into the next stage and on to the next identification connection level within 2–3 hops.

In table 1, we see that Resnet 50 is composed of the following components:

- A layer from convolution with 64 unique kernels and a stride of 2. The kernels have a size of 7 × 7.
- The next step is max pooling with a stride size of 2.
- That this next convolution has a 1 × 1,64 kernel, a 3 × 3,64 kernel, and a 1 ×1,256 kernel. This phase has nine layers because these three stages are performed three times in total.
- After that, there's a 1 × 1,128 kernels, 3 × 3,128 kernels, and 1 × 1,512 kernels. Four stages every time were repeated, totalling 12 of them.
- Following that, there are 1 × 1,256 kernels, followed by 3 × 3,256 and 1 × 1, 1024 kernels, all of which are duplicated six times for a total of 18 levels.
- There were 9 levels in total: a 1 × 1,512 kernel, a 3 × 3,512 kernel, and a 1 × 1,2048 kernel.
- After that, we conduct an averaged pool and conclude with a fully connected layer, accompanied by a softmax function, which results in a single line.

4. Experimental Results

- **Experimental Setup**

The suggested method has been implemented in the Python environment on an Intel Core i5 CPU running at 1.6 GHz. The recommended system was tested using the ADNI data set [17]. The Alzheimer's Disease Neuroimaging Initiative (ADNI) brings together specialists and research to better understand how Alzheimer's illness progresses (AD). Through MRI and PET imaging, genetics, cognitive tests, CSF, and blood biomarkers, ADNI researchers collect, validate, and use information as disease indicators. Along with Research materials and data from the North American ADNI project, this paper offers information about Alzheimer's disease, mild cognitive impairment, and ageing.

Simulation output:

As part of this study, 150 brain MRI images have been used to classify Alzheimer's disease patients into two categories: affected and unaffected.In the training phase, 75 images were used, and in the testing phase, 75 images.The results obtained by using the previously mentioned strategies are significantly more precise than those obtained by alternative techniques. Figure7 shows the input image.

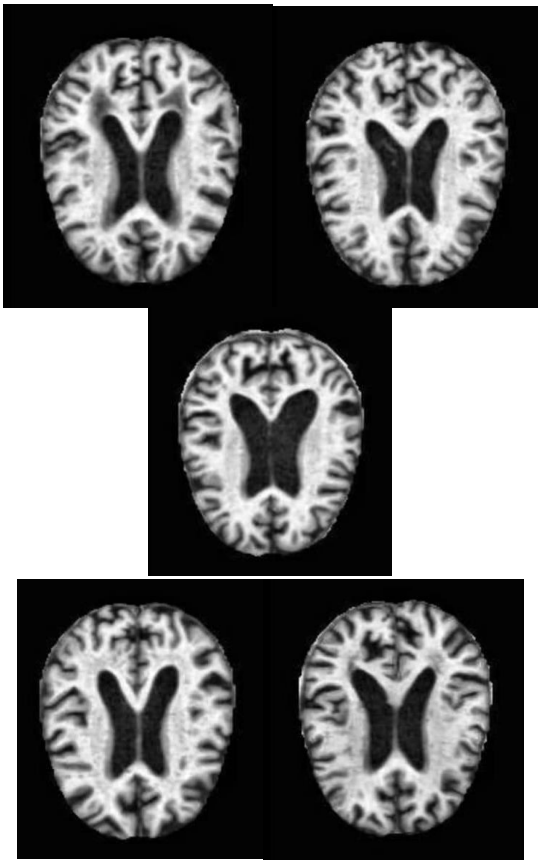

Figure 7: Samples from the ADNI dataset

Figure 8 illustrates how the input MRI Alzheimers images are preprocessed using the CLAHE and BADF algorithms, which provide greater image clarity after post-filtering, and less detail loss.The mean squared error (MSE), Peak Signal-to-Noise Ratio (PSNR) and structural similarity index (SSIM)are only a few of the performance measures listed in Table 2. If the MSE and PSNR are lower, the signal-to-noise ratio in the extracted image will be higher. The dice factor calculates how much overlap is there between the automatic and human segmentation process for a particular dataset.

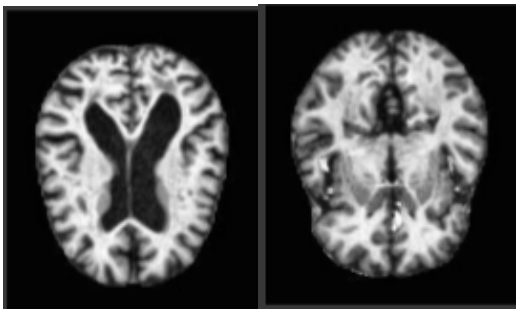

Figure 8: Preprocessed output

Table 2: Performance analysis of pre-processing results.

Filters	**CLAHE**				**BADF**			
Images	**MSE**	**PSNR**	**SNR**	**SSIM**	**MSE**	**PSNR**	**SNR**	**SSIM**
Sample 1	59.2	33.2	32.41	0.9751	55.1	35.66	37.41	0.9756
Sample 2	38.7	31.7	39.26	0.9733	33.57	36.17	40.26	0.9735
Sample 3	69.6	34.55	24.69	0.9735	59.76	35.45	29.69	0.9739
Sample 4	25.0	33.6	31.13	0.9760	20.07	36.66	34.1	0.9766
Sample 5	43.1	23.04	32.77	0.9742	41.17	36.04	37.7	0.9745
Sample 6	40.9	33.15	33.01	0.9743	30.91	36.10	39.71	0.9747

Segmentation is performed using the K-means algorithm after preprocessing.The various performance metrics of the segmentation process are detailed in Table 3. Dice Coefficient, Jaccard Coefficient, accuracy, and MCC (Matthews' correlation coefficient) are all assessed.

Table 3: Performance analysis of segmentation results.

	METRICS	**K-means clustering**
Image 1	*Dice Coefficient*	0.7964
	Jaccard Coefficient	0.6617
	MCC	0.8117
	Accuracy(%)	0.9957
Image 2	*Dice Coefficient*	0.9088
	Jaccard Coefficient	0.8328
	MCC	0.9114
	Accuracy	0.9974
Image 3	*Dice Coefficient*	0.9818
	Jaccard Coefficient	0.9642
	MCC	0.9814
	Accuracy	0.9991
Image 4	*Dice Coefficient*	0.7846
	Jaccard Coefficient	0.6456
	MCC	0.7647
	Accuracy	0.9989

Images with unclear boundaries are separated by k-Means clustering.In most cases, these are used to define Alzheimer's region shapes.Marking severity in this way will be efficient. As can be seen in Table 4, this algorithm is used to calculate the area parameter centroid diameter.

Table 4: Calculation of The area parameter centroid diameter

Samples	**K-mean clustering**		
	Mean	***Variance***	***Standard error***
1	0.582031	0.460936	0.020371
2	0.694118	0.49991	0.025185
3	0.740741	0.496041	0.023866
4	0.705078	0.455954	0.02015
5	0.582031	0.460936	0.020371

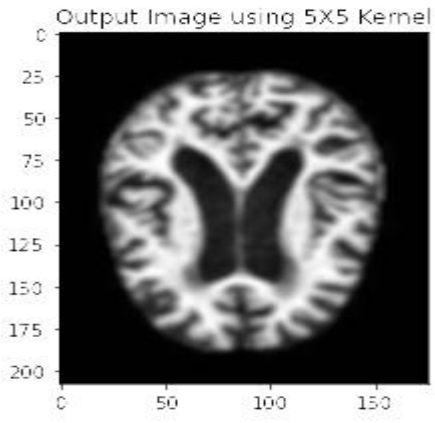

Figure 9: Classification output

The updated ResNet-50 architecture has been used in the suggested framework for extracting features, identification, and categorization of MRI images on Alzheimer's disease. Figure 9 depicts the detection and classification output, the statistical value under the output represents the probability of positive as well as the probability of negative outputs. Thus the proposed framework is accurately identifying the affected and non-affected MRI images.

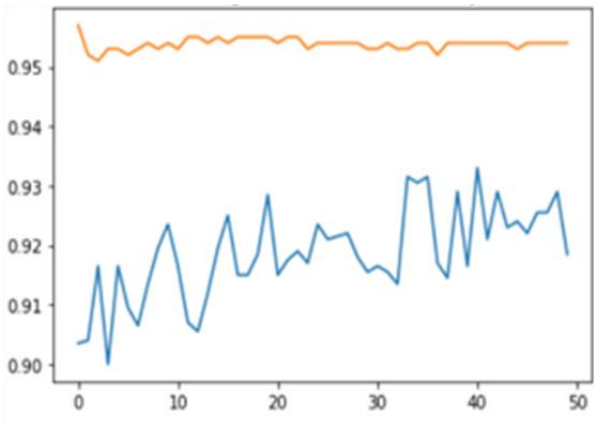

Figure 10:Training and validation accuracy

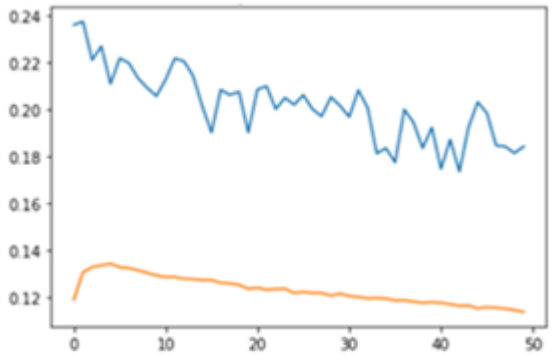

Figure 11: Training and validation loss

The proposed system of Alzheimer's disease identification has training and validation accuracy, as shown in Figure 10. It's worth noting that testing precision exceeds 95%, while validation precision hovers around 93%. In this figure, the blue colour indicates the validation and the red colour indicates the training. The suggested architecture for Alzheimer's disease identification also suffers from training and validation loss, as seen in Figure 11.It is worth noticing that the proposed system obtains the minimum training and validation losses as around 0.12 and 0.20 respectively.In this figure, the blue colour indicates the validation and the red colour indicates the loss. Table5 shows the accuracy, sensitivity, and specificity performance measures of the proposed model compared to the existing model.

Table 5: Comparison of performance metrics

References	Accuracy	Sensitivity	Specificity
[23]	93.01	89.13	96.8
[24]	91.02	92.7	89.05
[25]	91.95	89.5	93.8
[26]	92	90.9	93
[27]	91.41	89.06	93.75
[28]	94.7	94.3	95.8
Proposed	***95.9***	***96.2***	***97.4***

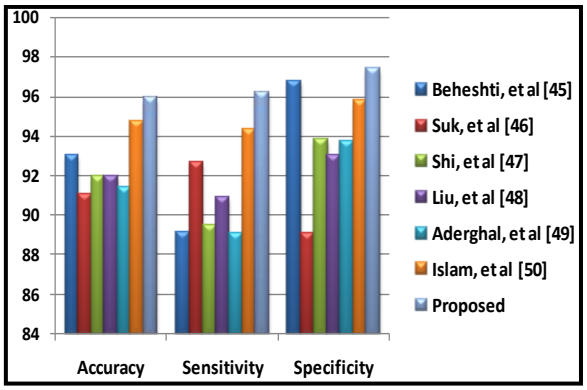

Figure 12: Comparison of performance metrics

Based on the performance parameters such as accuracy, sensitivity, and specificity our proposed framework[45-50], is compared with other existing techniques. Figure12 depicts the graphical depiction, and table 5 shows the statistical representation. We can see from the table and graph that the proposed framework outperforms strategic approaches for detecting and classifying Alzheimer's disease.

5. Conclusion

MRI has evolved in neurology and oncology over the last several years.MRI has improved soft tissue delineation, which makes it the most commonly used imaging technique in the early stages of primary Alzheimer's illness. Researchers used Resnet 50, a deep-learning technique previously used to diagnose Alzheimer's illness.The results suggested that the deep learning based ResNet 50 is promising for classification and diagnosing diseases with neuroimaging data. The proposed method uses K-means clustering to extract regions of interest from MR Images.Utilizing standard datasets, we test the proposed model's performance and categorize MRI as normal AD.As a result, it produces more precise results with greater efficiency.

References

[1] Zetterberg, Henrik, and Barbara B. Bendlin. "Biomarkers for Alzheimer's disease—preparing for a new era of disease-modifying therapies." *Molecular psychiatry* 26, no. 1 (2021): 296-308.

[2] Sanchez, Justin S., J. Alex Becker, Heidi IL Jacobs, Bernard J. Hanseeuw, Shu Jiang, Aaron P. Schultz, Michael J. Properzi et al.

"The cortical origin and initial spread of medial temporal tauopathy in Alzheimer's disease assessed with positron emission tomography." *Science translational medicine* 13, no. 577 (2021): eabc0655.

[3] Johansson, Maurits, Erik Stomrud, Philip S. Insel, Antoine Leuzy, Per Mårten Johansson, Ruben Smith, Zahinoor Ismail et al. "Mild behavioural impairment and its relation to tau pathology in preclinical Alzheimer's disease." *Translational psychiatry* 11, no. 1 (2021): 1-8.

[4] Leng, Kun, Emmy Li, Rana Eser, Antonia Pierogies, Rene Sit, Michelle Tan, Norma Neff et al. "Molecular characterization of selectively vulnerable neurons in Alzheimer's disease." *Nature neuroscience* 24, no. 2 (2021): 276-287.

[5] Wightman, Douglas P., Iris E. Jansen, Jeanne E. Savage, Alexey A. Shadrin, Shahram Bahrami, Dominic Holland, ArvidRongve et al. "A genome-wide association study with 1,126,563 individuals identifies new risk loci for Alzheimer's disease." *Nature genetics* 53, no. 9 (2021): 1276-1282.

[6] Nguyen, Phuong H., AyyalusamyRamamoorthy, Bikash R. Sahoo, Jie Zheng, Peter Faller, John E. Straub, Laura Dominguez et al. "Amyloid oligomers: A joint experimental/computational perspective on Alzheimer's disease, Parkinson's disease, type II diabetes, and amyotrophic lateral sclerosis." *Chemical reviews* 121, no. 4 (2021): 2545-2647.

[7] Karikari, Thomas K., Andrea L. Benedet, Nicholas J. Ashton, Juan Lantero Rodriguez, AnniinaSnellman, Marc Suarez-Calvet, Paramita Saha-Chaudhuri et al. "Diagnostic performance and prediction of clinical progression of plasma phosphor-tau181 in the Alzheimer's Disease Neuroimaging Initiative." *Molecular psychiatry* 26, no. 2 (2021): 429-442.

[8] Neff, Ryan A., Minghui Wang, SezenVatansever, Lei Guo, Chen Ming, Qian Wang, Erming Wang et al. "Molecular subtyping of Alzheimer's disease using RNA sequencing data reveals novel mechanisms and targets." *Science advances* 7, no. 2 (2021): eabb5398.

[9] Qiu, Chengxuan, MiiaKivipelto, and Eva Von Strauss. "Epidemiology of Alzheimer's disease: occurrence, determinants, and strategies toward intervention." *Dialogues in clinical neuroscience* (2022).

[10] Dubois, Bruno, Gaetane Picard, and Marie Sarazin. "Early detection of Alzheimer's disease: new diagnostic criteria." *Dialogues in clinical neuroscience* (2022).

[11] Gao, Shuangshuang, and Dimas Lima. "< PE-AT> A review of the application of deep learning in the detection of Alzheimer's disease." *International Journal of Cognitive Computing in Engineering* (2021).

[12] Attallah, Omneya, Maha A. Sharkas, and HebaGadelkarim. "Deep learning techniques for automatic detection of embryonic neurodevelopmental disorders." *Diagnostics* 10, no. 1 (2020): 27.

[13] Liu, Fei, Huabin Wang, Yonglin Chen, Yu Quan, and Liang Tao. "Convolutional neural network based on feature enhancement and attention mechanism for Alzheimer's disease prediction using MRI images." In *Proc. of SPIE Vol*, vol. 12083, pp. 120830X-1. 2022.

[14] Loddo, Andrea, Sara Buttau, and Cecilia Di Ruberto. "Deep learning based pipelines for Alzheimer's disease diagnosis: a comparative study and a novel deep-ensemble method." *Computers in biology and medicine* 141 (2022): 105032.

[15] A. Kaur and C. Singh, "Contrast enhancement for cephalometric images using wavelet-based modified adaptive histogram equalization," Applied Soft Computing, vol. 51, pp. 180–191, 2017.

[16] Shehroz S. Khan and Amir Ahmad, Cluster Centre Initialization Algorithm for *K*-means Cluster, In *Pattern Recognition Letters*, pp. 1293–1302, (2004).

[17] D. Sonker, "Comparison of Histogram Equalization Techniques for Image Enhancement of Grayscale images in Natural and Unnatural light," International Journal of Engineering Research and Development, vol. 8, no. 9, pp. 57–61, 2013.

[18] Pizer SM, et.al (1990) "Contrast-limited adaptive histogram equalization: speed and effectiveness", In Proceedings of the first conference on visualization in biomedical computing. IEEE, pp 337–345.

[19] Aimi Salihai Abdul, MohdYusuffMasor and Zeehaida Mohamed, Colour Image Segmentation Approach for Detection of Malaria Parasite using Various Colour Models and *k*-Means Clustering, In *WSEAS Transaction on Biology and Biomedicine.*, vol. 10, January (2013).

[20] Hossain, Md Belal, SM Hasan Sazzad Iqbal, Md Monirul Islam, Md Nasim Akhtar, and Iqbal H. Sarker. "Transfer learning with fine-tuned deep CNN ResNet50 model for classifying COVID-19 from chest X-ray images." *Informatics in Medicine Unlocked* (2022): 100916.

[21] .Alsabhan, Waleed, and TurkyAlotaiby. "Automatic Building Extraction on Satellite Images Using Unet and ResNet50." *Computational Intelligence and Neuroscience* 2022 (2022).

[22] Saadna, Youness, AnouarAbdelhakimBoudhir, and Mohamed Ben Ahmed. "An Analysis of ResNet50 Model and RMSprop Optimizer for Education Platform Using an Intelligent Chatbot System." In *Networking, Intelligent Systems and Security*, pp. 577-590. Springer, Singapore, 2022.

[23] Beheshti, I., Demirel, H., Matsuda, H., Initiative, A.D.N., et al.: Classification of Alzheimer's disease and prediction of mild cognitive impairment-to-Alzheimer's conversion from structural magnetic resource imaging using feature ranking and a genetic algorithm. Comput. Biol. Med. 83, 109–119 (2017).

[24] Suk, H.I., Lee, S.W., Shen, D.: Deep ensemble learning of sparse regression models for brain disease diagnosis. Med. Image Anal. 37, 101–113 (2017).

[25] Shi, B., et al.: Nonlinear feature transformation and deep fusion for Alzheimer's disease staging analysis. Pattern Recognit. 63, 487–498 (2017).

[26] Liu, M., Zhang, D., Shen, D., Alzheimer's Disease Neuroimaging Initiative: Hierarchical fusion of features and classifier decisions for Alzheimer's disease diagnosis. Hum. Brain Mapp. 35(4), 1305–1319 (2014).

[27] Aderghal, K., Benois-Pineau, J., Afdel, K.: Classification of SMRI for Alzheimer's disease diagnosis with CNN: single Siamese networks with 2d+? approach and fusion on ADNI. In: Proceedings of the 2017 ACM on International Conference on Multimedia Retrieval, pp. 494–498. ACM (2017).

[28] Islam, Jyoti, Yanqing Zhang, and Alzheimer's Disease Neuroimaging Initiative. "Deep convolutional neural networks for automated diagnosis of Alzheimer's disease and mild cognitive impairment using 3D brain MRI." In International Conference on Brain Informatics, pp. 359-369. Springer, Cham, 2018.